ORIGINAL RESEARCH

Inhalation of *Stachybotrys chartarum* Fragments Induces Pulmonary Arterial Remodeling

Tara L. Croston[1], Angela R. Lemons[1], Mark A. Barnes[1], William T. Goldsmith[2], Marlene S. Orandle[3], Ajay P. Nayak[1,4], Dori R. Germolec[5], Brett J. Green[1], and Donald H. Beezhold[6]

[1]Allergy and Clinical Immunology Branch, [2]Engineering and Control Technology Branch, [3]Pathology and Physiology Research Branch, and [6]Office of the Director, Health Effects Laboratory Division, National Institute for Occupational Safety and Health, Centers for Disease Control and Prevention, Morgantown, West Virginia; [4]Department of Medicine, Center for Translational Medicine and Division of Pulmonary, Allergy and Critical Care Medicine, and Jane and Leonard Korman Respiratory Institute, Thomas Jefferson University, Philadelphia, Pennsylvania; and [5]Toxicology Branch, National Toxicology Program Division, National Institute of Environmental Health Sciences, Durham, North Carolina

Abstract

Stachybotrys chartarum is a fungal contaminant within the built environment and a respiratory health concern in the United States. The objective of this study was to characterize the mechanisms influencing pulmonary immune responses to repeatedly inhaled *S. chartarum*. Groups of B6C3F1/N mice repeatedly inhaled viable trichothecene-producing *S. chartarum* conidia (strain A or strain B), heat-inactivated conidia, or high-efficiency particulate absolute–filtered air twice per week for 4 and 13 weeks. Strain A was found to produce higher amounts of respirable fragments than strain B. Lung tissue, serum, and BAL fluid were collected at 24 and 48 hours after final exposure and processed for histology, flow cytometry, and RNA and proteomic analyses. At 4 weeks after exposure, a T-helper cell type 2–mediated response was observed. After 13 weeks, a mixed T-cell response was observed after exposure to strain A compared with a T-helper cell type 2–mediated response after strain B exposure. After exposure, both strains induced pulmonary arterial remodeling at 13 weeks; however, strain A–exposed mice progressed more quickly than strain B–exposed mice. BAL fluid was composed primarily of eosinophils, neutrophils, and macrophages. Both the immune response and the observed pulmonary arterial remodeling were supported by specific cellular, molecular, and proteomic profiles. The immunopathological responses occurred earlier in mice exposed to high fragment-producing strain A. The rather striking induction of pulmonary remodeling by *S. chartarum* appears to be related to the presence of fungal fragments during exposure.

Keywords: *Stachybotrys chartarum* fungal fragmentation; pulmonary arterial remodeling; fungal exposure

Clinical Relevance

Stachybotrys chartarum, or black mold, is found in damp indoor environments and is a respiratory health concern in the United States. Two strains of *S. chartarum* were used in the present study, with one strain fragmenting to a greater extent. Repeated exposure resulted in inflammation and pulmonary arterial remodeling and suggested that the presence of fungal fragments induced an earlier response.

(Received in original form June 18, 2019; accepted in final form October 30, 2019)

Supported in part by an interagency agreement between the National Institute for Occupational Safety and Health (NIOSH) and the National Institute of Environmental Health Sciences (AES12007001-1-0-6) as a collaborative National Toxicology Program research activity. This study was also funded in part by Centers for Disease Control and Prevention/NIOSH intramural funds (927ZLCT). The findings and conclusions in this study are those of the authors and do not necessarily represent the official position of NIOSH, Centers for Disease Control and Prevention.

Author Contributions: T.L.C., A.R.L., A.P.N., B.J.G., and D.H.B. conceived of and designed the research. T.L.C., A.R.L., and A.P.N. cultured the test articles. W.T.G. conducted the exposures. T.L.C., A.R.L., M.A.B., and A.P.N. performed the experiments. T.L.C. and M.A.B. analyzed the data. T.L.C., M.S.O., B.J.G., and D.H.B. interpreted results of the experiments. T.L.C., A.R.L., M.A.B., and M.S.O. prepared the figures. T.L.C. drafted the manuscript. T.L.C., A.R.L., M.A.B., M.S.O., A.P.N., D.R.G., B.J.G., and D.H.B. edited and revised the manuscript. T.L.C., A.R.L., M.A.B., W.T.G., M.S.O., A.P.N., D.R.G., B.J.G., and D.H.B. approved the final version of the manuscript.

Correspondence and requests for reprints should be addressed to Tara L. Croston, Ph.D., Allergy and Clinical Immunology Branch, Health Effects Laboratory Division, National Institute for Occupational Safety and Health, Centers for Disease Control and Prevention, 1095 Willowdale Road, Morgantown, WV 26505. E-mail: xzu9@cdc.gov.

This article has a related editorial.

This article has a data supplement, which is accessible from this issue's table of contents at www.atsjournals.org.

Am J Respir Cell Mol Biol Vol 62, Iss 5, pp 563–576, May 2020

Originally Published in Press as DOI: 10.1165/rcmb.2019-0221OC on October 31, 2019
Internet address: www.atsjournals.org

Fungal contamination in indoor environments is a public health concern in the United States. Indoor fungal bioaerosols are generated by fungal disturbances, such as vibrations or airflow through contaminated areas within buildings, and exposure to fungal bioaerosols has been associated with human disease (1, 2). Among species that are frequently observed, *Stachybotrys chartarum* exposure has become an area of heightened interest. Since a case study in 1994 identified *S. chartarum* as a potential cause of acute idiopathic pulmonary hemosiderosis among infants (3, 4), evidence has accumulated for the epidemiologic association of *S. chartarum* with health effects; however, this association with acute idiopathic pulmonary hemosiderosis is less convincing (5). Although recent consensus documents have confirmed associations between damp indoor environments and adverse respiratory symptoms (1, 2), the contribution of *S. chartarum* to adverse pulmonary immune responses requires further delineation.

S. chartarum is a black, macroscopic, saprophytic, filamentous fungus that requires high amounts of moisture and cellulose for optimal growth (6–8). *S. chartarum* spores are ~3–6 μm in diameter and produce mycotoxins (9, 10) and allergens (11, 12). There are several chemotypes of *S. chartarum*, including macrocyclic trichothecene-producing and atranone-producing strains. Although this fungus has toxigenic properties, the fungal components common to other fungal species are believed to be more critical to its pathophysiology (13–16).

Fungal bioaerosols are composed of aerosolized fungal spores and fragments. These fragments are derived from fragmented spores or hyphae and have been shown to aerosolize in higher concentrations than spores (17). *S. chartarum* has previously been shown to fragment (18, 19); however, the influence of *S. chartarum* fungal fragment exposure has not been fully elucidated. The present study used two different *S. chartarum* strains that included a high-fragmenting isolate and a low-fragmenting isolate. Aerosolized *S. chartarum* was repeatedly delivered to mice housed in a nose-only chamber to more closely mimic natural human exposure, a documented methodological advancement over studies using intranasal instillations, intratracheal instillations, or liquid aerosol inhalations (20–26). This model has been validated by characterizing the immune response and genetic profile after *Aspergillus fumigatus* exposure (27–29).

Previous data from our laboratory and others demonstrate pulmonary pathology after *S. chartarum* exposure (24, 25, 30, 31); however, the underlying mechanisms need further clarification. The aim of this study was to characterize the mechanisms contributing to the pulmonary immune responses after repeated exposure to *S. chartarum*. Two different strains of *S. chartarum* exhibiting varying degrees of fragmentation were individually employed. After exposure, lung tissue, serum, and BAL fluid (BALF) were collected at 24 and 48 hours after final exposure and processed for histology, flow cytometry, and RNA and proteomic analyses to characterize immune mechanisms. The use of the two strains that fragmented to a varying extent helped to differentiate the role of fungal fragmentation in the development of immune response and disease pathology.

Methods

Fungal Cultures

The two macrocyclic trichothecene-producing strains of *S. chartarum* used in this study were IBT 9460 (strain A) and IBT 7711 (strain B). Strain A produced sixfold higher concentrations of verrucarol and fragmented to a greater extent (<0.5–2 μm in aerodynamic diameter) compared with strain B (Figure 1). Fungal test articles were aerosolized using a computer-controlled acoustical generator system as previously documented (28). *See* Data Supplement E1 for further details.

Animals

Female B6C3F1/N mice, 5–6 weeks old, were acquired from the National Toxicology Program mouse colony housed at Taconic Biosciences, Inc. Mice were housed in the Assessment and Accreditation of Laboratory Animal Care International–accredited animal facility at the National Institute for Occupational Safety and Health (NIOSH) and were provided an NTP-2000 diet (Harlan Laboratories) and water *ad libitum*. The mice appeared healthy throughout the study (Figure E2 in the data supplement). All animal procedures were performed under a NIOSH Animal Care and Use Committee–approved protocol.

Fungal Exposures

Mice were randomly separated into six exposure groups with 15 mice per group: Groups 1 and 2 were *S. chartarum* strain A, viable or heat-inactivated conidia (HIC); groups 3 and 4 were *S. chartarum* strain B, viable or HIC; and groups 5 and 6 were control groups of high-efficiency particulate absolute–filtered air only. The *S. chartarum*–exposed mice inhaled 1×10^4 particles (estimated pulmonary deposition/exposure), which was the highest aerosolized dose that reproducibly

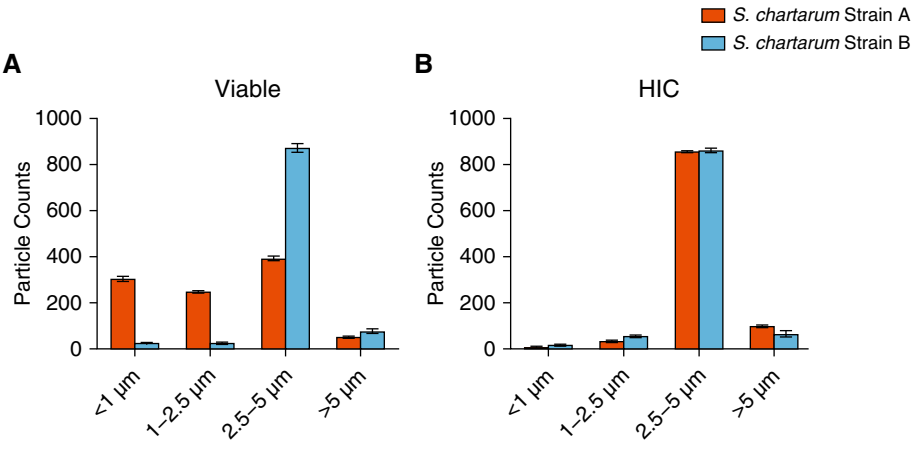

Figure 1. Fragmentation of *Stachybotrys chartarum*. Aerodynamic particle size distributions of (*A*) viable and (*B*) heat-inactivated *S. chartarum* conidia (HIC) collected during exposures. Data are a representation of the particle size distribution observed over multiple exposures and have been normalized to 1,000 particle counts for comparison. *S. chartarum* = *Stachybotrys chartarum*.

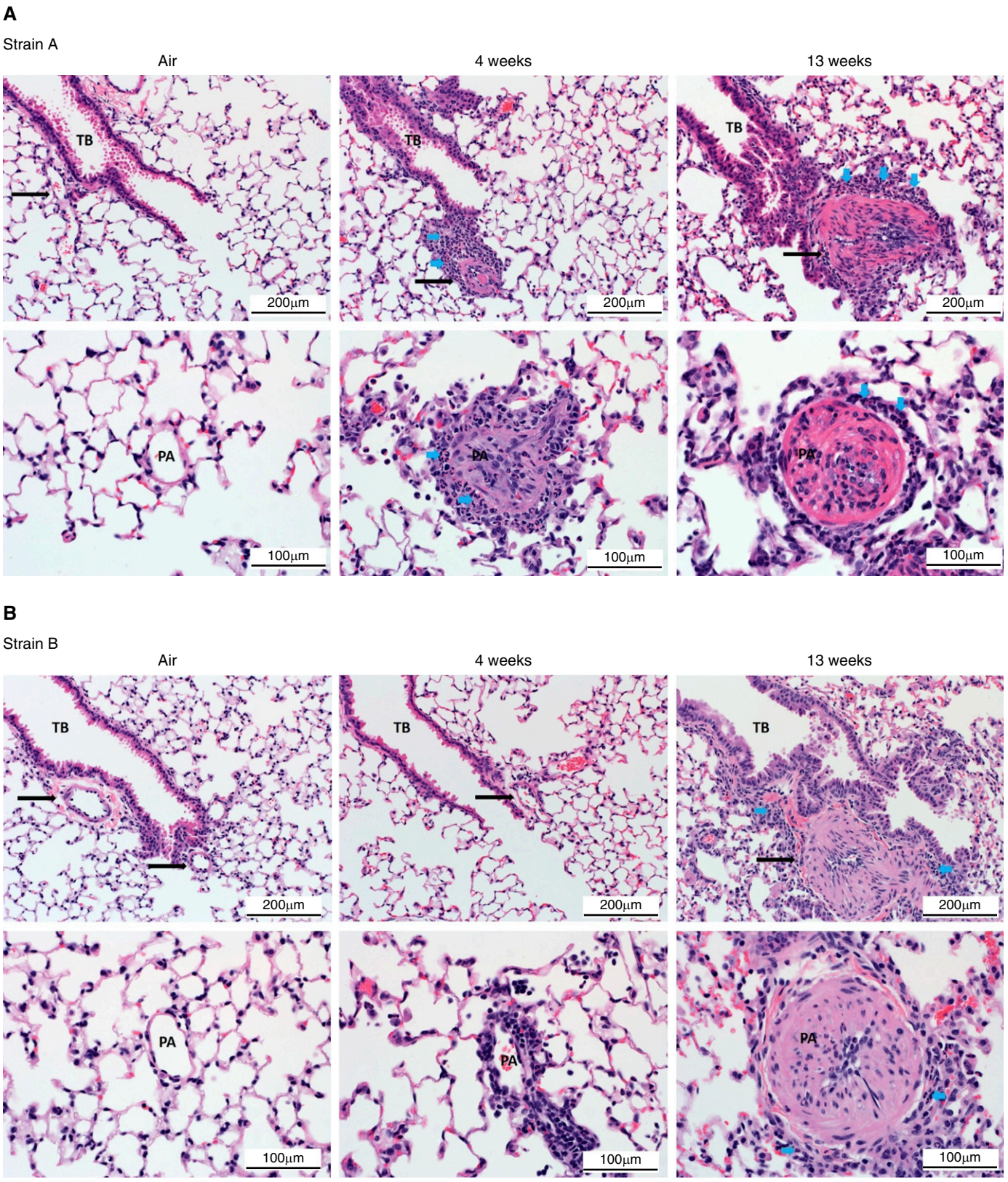

Figure 2. Pulmonary arterial remodeling. Representative photomicrographs of hematoxylin and eosin–stained sections of lung from mice exposed to viable (*A*) strain A and (*B*) strain B. The mice were killed at 24 hours after 4 or 13 weeks of exposure. Lung from an air-exposed mouse is shown for reference. (*C*) Representative photomicrographs showing the range of changes seen in pulmonary arteries in lungs of mice exposed to viable fungal conidia. The blue arrows indicate different inflammatory cells (i.e., eosinophils and macrophages). Scale bars: 200 μm and 100 μm. PA = pulmonary arteries (indicated by black arrows); TB = terminal bronchiole.

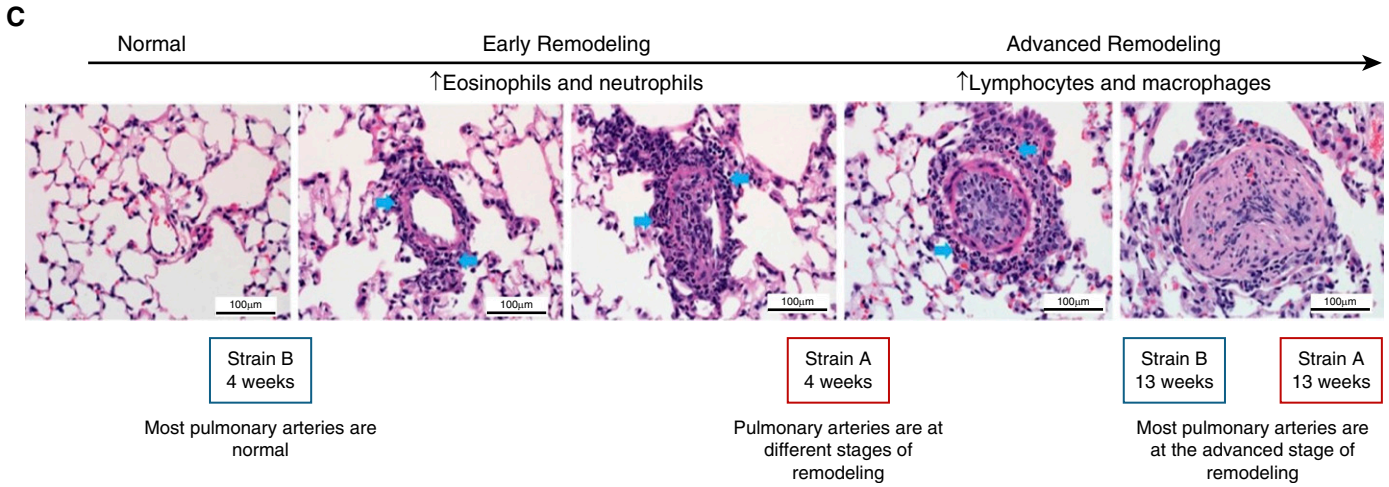

Figure 2. (Continued)

induced a lymphoproliferative response. Mice were exposed twice per week for 4 or 13 weeks as previously documented (28). Samples were collected 24 hours and 48 hours after final exposure to assess temporal changes in immune responses. Mice were killed via intraperitoneal injection of 200 mg/kg sodium pentobarbital solution (Fatal-Plus Solution; Vortech Pharmaceuticals, Ltd.) and exsanguinated via cardiac puncture. The exposure scheme and harvesting time points were chosen on the basis of preliminary immune response data (27, 29).

Histopathology

Left lung lobes ($n = 3$/group) were inflated with fixative and collected. The tissue was then embedded, sectioned, and stained with hematoxylin and eosin for routine histopathological evaluation as previously described (29). For additional details, *see* Data Supplement E2.

Flow Cytometric and Cell Differential Analyses

Cells collected from BAL ($n = 7$/group) were enumerated using a Cellometer Vision (Nexcelom Bioscience) and prepared for flow cytometric analysis as previously described (29). Cells were blocked and stained using fluorochrome-conjugated antibodies (Table E1). *See* Data Supplement E3 for additional details.

Proteomic and RNA Analyses

Right lung lobes ($n = 3$/group) were sent to MS Bioworks for quantitative proteomic analysis as previously described (29). Total RNA was extracted for microRNA (miRNA) (Exiqon Services) and mRNA analyses as previously described (28). Additional analyzed genes are reported in Table E2. T-helper cell type 1 (Th1), Th2, and Th17 gene expression data were normalized to *gusb* (β-glucuronidase) and additional genes to *gapdh* (glyceraldehyde 3-phosphate dehydrogenase).

Proteomic and RNA data were analyzed by using Ingenuity Pathway Analysis (IPA) software (Qiagen) for core, comparative, and miRNA target filter analyses (28). For additional details, *see* Data Supplement E4.

Statistics

Statistical power tests were conducted to determine the appropriate number of samples needed for each endpoint measurement. Fold changes greater than or equal to 2 or less than or equal to −2 were considered altered. $P \leq 0.05$ was considered statistically significant (28, 29). *See* Data Supplement E5 for additional details.

Results

Histopathological Assessment

Inflammation and arterial remodeling were observed in murine lungs after repeated exposure to viable *S. chartarum* (Figure 2). Differences in lesion development

Table 1. Summary of Observations from Mice Exposed to Viable *Stachybotrys chartarum*

	Arterial Remodeling				Airway Changes		Alveolar Changes	
	Early	Continuum	Advanced	Thrombi	Inflammation	Mucous Metaplasia	Histiocytosis	M2 Histiocytosis
4 wk								
Strain A	0/6	3/6	2/6	4/6	5/6	5/6	5/6	0/6
Strain B	3/6	2/6	0/6	0/6	4/6	0/6	0/6	0/6
13 wk								
Strain A	0/6	0/6	6/6	2/6	6/6	6/6	1/6	5/6
Strain B	0/6	1/6	5/6	2/6	5/6	5/6	2/6	4/6

Lungs ($n = 3$/group) from 24- and 48-hour time points were pooled together for $n = 6$.

between the two strains were most evident microscopically after 4 weeks (Table 1). No microscopic changes were observed in lungs exposed to HIC or high-efficiency particulate absolute–filtered air controls (Figure E2).

At 4 weeks, strain A exposure produced a robust peribronchiolar and perivascular inflammatory response characterized by eosinophilic and neutrophilic infiltrates centered at terminal bronchioles with extension into adjacent alveoli (Figure 2A). Similar inflammatory cells were also observed surrounding smaller pulmonary arteries and within the vessel wall. Remodeling of pulmonary arteries near the terminal bronchiole was evident after 4 weeks of exposure to strain A (Figure 2A). Additional histological changes observed after 4-week strain A exposure included alveolar histiocytosis, bronchiolar epithelial cell hyperplasia with mucous metaplasia, and vascular thrombi (Table 1), whereas strain B exposure resulted in minimal airway inflammation (Figure 2B).

After 13 weeks of exposure, histopathology was nearly indistinguishable between the two strains. Bronchiolitis and pulmonary arterial remodeling were observed in the lungs; however, there was a shift in inflammatory cell composition from eosinophils and neutrophils at 4 weeks to lymphocytes and macrophages at 13 weeks (Figures 2A and 2B), indicating the mice were further along in the pulmonary arterial remodeling process.

A summary of the histopathology showing a continuum of microscopic changes ranging from arteritis to pulmonary arterial remodeling is presented in Figure 2C. Early changes in pulmonary arteries were characterized by inflammation, whereas later changes in vessels were more severe and characterized by arterial remodeling. Remodeling in affected vessels was characterized by symmetrical thickening of the artery wall and narrowing of the lumen, affecting the small to medium-sized vessels at or below the level of the terminal bronchiole. With increasing exposure duration, there was a shift in inflammatory cell types from polymorphonuclear cells to mononuclear cells.

Flow Cytometry

The BALF was composed primarily of eosinophils, neutrophils, and macrophages (Figure 3). Compared with air-only controls, strain A exposure showed increased eosinophils and neutrophils 24 hours after 4 and 13 weeks (Figures 3A and 3B). Alveolar macrophages were significantly increased 48 hours after 13-week strain A exposure (Figure 3C). Only after 4-week strain A HIC exposure were eosinophils, neutrophils, and alveolar macrophages initially increased (Figures 4A–4C).

Strain B–exposed mice showed significantly increased eosinophils and alveolar macrophages 48 hours after 4-week exposure (Figures 3D and 3F). After 13-week exposure, eosinophils, neutrophils, and alveolar macrophages were significantly increased (Figures 3D–3F). Strain B HIC exposure did not result in significant cell population changes (Figures 4D–4F).

Quantitative Proteomic Analysis

Proteomic analysis of whole-lung homogenate detected 3,465 proteins in total (Table E3). Table 2 shows differentially expressed proteins involved in tissue remodeling and inflammation. Chil3 and chil4 (chitinase-like proteins 3 and 4, respectively) were upregulated after 4-week

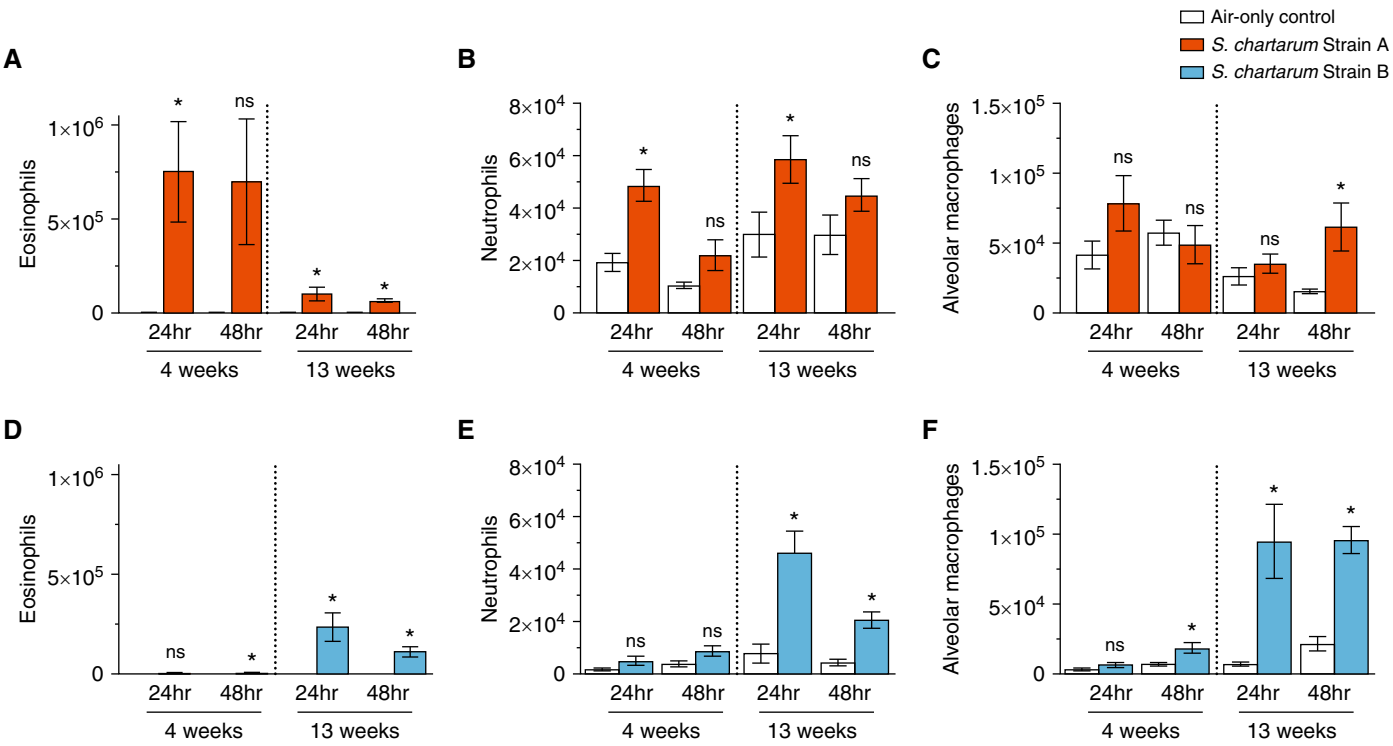

Figure 3. Cell populations of BAL fluid (BALF) after exposure to strain A and strain B. (*A–F*) BALF collected at 24 and 48 hours after 4- and 13-week exposures to strain A (*A–C*) or strain B (*D–F*) consisted of eosinophils (*A* and *D*), neutrophils (*B* and *E*), and macrophages (*C* and *F*). Values are expressed as mean ± SEM; $n = 7$ per group. *$P \leq 0.05$ for exposed group versus air-only control group. ns = not significant.

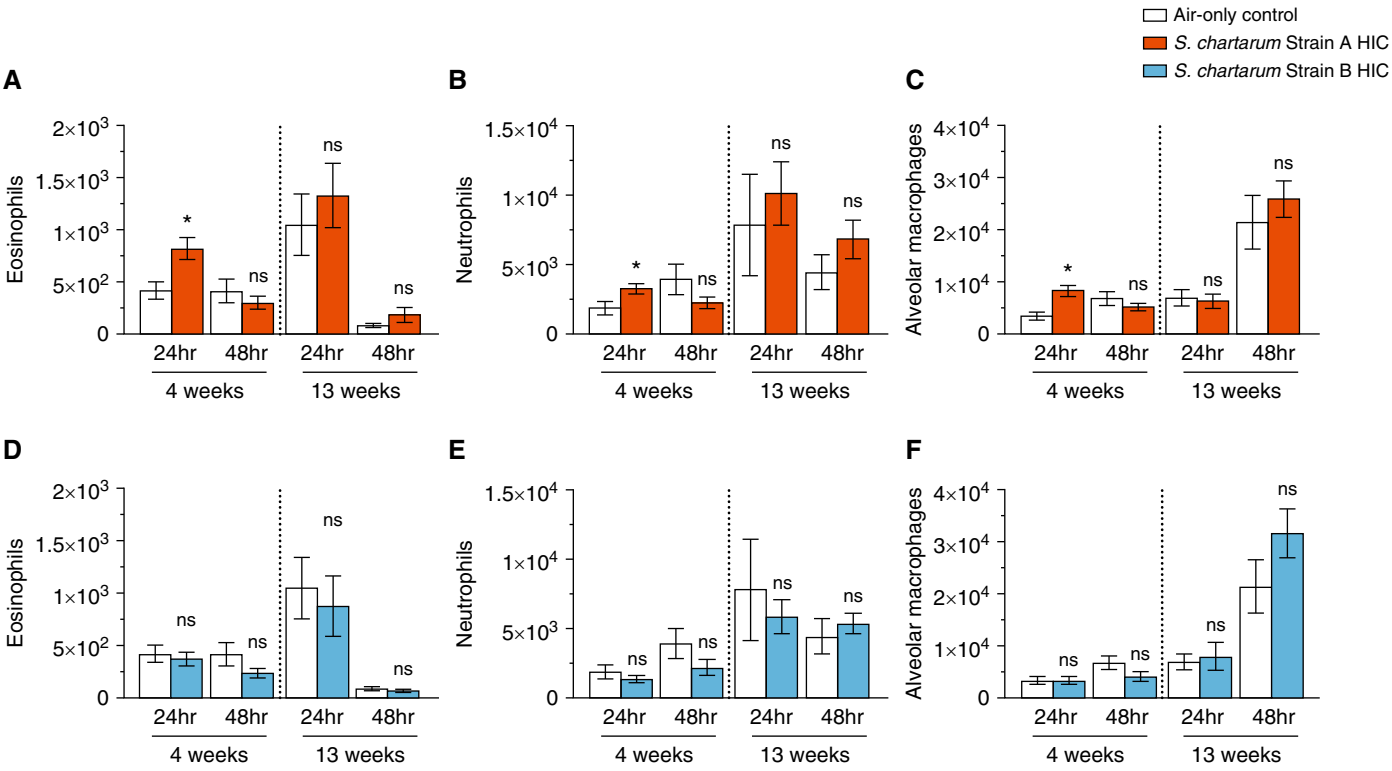

Figure 4. Cell populations of BAL fluid after exposure to strain A HIC and strain B HIC. (*A–F*) BALF collected at 24 and 48 hours after a 4- and 13-week exposure to strain A HIC (*A–C*) or strain B HIC (*D–F*) consisted of eosinophils (*A* and *D*), neutrophils (*B* and *E*), and macrophages (*C* and *F*). Values are expressed as mean ± SEM; $n = 7$ per group. *$P \leq 0.05$ for exposed group versus air-only control group.

and 13-week strain A exposures, but only after 13-week strain B exposure. Only chil3 was decreased after 4-week strain A HIC exposure. Lgals3 (galectin-3) was upregulated after 4-week and 13-week strain A exposures. After 4-week strain B exposure, lgals3 was decreased, but it was increased after 13 weeks. In contrast, lgals3 was downregulated after 4-week strains A and B HIC exposure. Von Willebrand factor was upregulated after 13-week strain A exposure but downregulated after strain B exposure. Strains A and B HIC exposure resulted in a downregulation of von Willebrand factor after 4-week exposure. Strain A–exposed mice showed increased sftpa (pulmonary surfactant protein A) after 4-week and 13-week exposures. In contrast, both sftpa and sftpd were decreased after 4-week strain B exposure and after 4-week strains A and B HIC exposure.

Inflammation-associated proteins retnla (resistin-like α) and mrc1 (macrophage mannose receptor 1) were significantly increased after 4-week and 13-week strain A exposures. After 13-week strain B exposure, retnla was upregulated. Although mrc1 was downregulated at 4 weeks, expression was slightly increased after 13-week strain B exposure. Retnla was unaltered in mice exposed to either HIC strain; however, mrc1 was decreased after 4-week strains A and B HIC exposure. Located in the eosinophil matrix, ear1 and ear2 (eosinophil cationic proteins 1 and 2 receptors, respectively) were significantly increased after 4-week strain A exposure. After 13 weeks, both ear1 and ear2 were increased over 100-fold at 48 hours. With strain B, ear1 and ear2 were only upregulated after 13-week exposure, but not to the same degree as with strain A. For HIC exposures, ear1 and ear2 were decreased after 4-week strain A exposure, and ear1 was decreased after 13-week strain B exposure.

Carbohydrate-binding clec proteins (C-type lectins) are nonspecific pathogen recognition receptors. After strain A exposure, clec7a and clec10a were increased after 4 weeks, and after 13 weeks, clec10a and clec3b were increased. Strain B–exposed mice showed increased clec7a after 4 weeks and increased clec10a after 13 weeks. Unaltered after strain A HIC exposure, clec7a was decreased after 4-week strain B HIC exposure. Clec3b was also decreased after 4-week strains A and B HIC exposure.

Core proteomic analysis conducted using IPA identified associations between altered proteins and canonical pathways, diseases and disorders, and physiological system development and functions, as well as the top cardiotoxicity pathways. These top relationships, mechanisms, functions, and pathways relevant to a dataset are determined by having the highest number of proteins that overlap those included in the specific pathway, disease, or function. As reported in Tables 3 and 4, one of the top canonical pathways identified after exposure to strain A is eIF2 (eukaryotic initiation factor 2) signaling, a component of protein synthesis. After strain A exposure, organismal injury and abnormalities were identified as the top diseases and disorders at all time points, followed by the inflammatory response and neurological disease. The top physiological system developments and functions

Table 2. Alterations in Proteomic Profiles

Proteins	Symbol	Strain A				Strain B			
		4 wk		13 wk		4 wk		13 wk	
		24 h	48 h	24 h	48 h	24 h	48 h	24 h	48 h
Viable									
Chitinase-like protein 3	chil3	14.8*	—	—	157.7*	—	—	149.0*	77.6*
Chitinase-like protein 4	chil4	129.5*	—	171.8*	860.1*	—	—	98.1*	—
Galectin-3	lgals3	2.1*	—	8.0*	15.1*	—	−2.0*	—	2.7*
Von Willebrand factor	vWF	—	—	2.3*	—	—	−2.3	—	—
Resistin-like α	retnla	NC*	—	—	NC*	—	—	87.4*	NC*
Macrophage mannose receptor 1	mrc1	3.5*	—	3.7*	7.5*	—	−2.1*	2.1*	—
Eosinophil cationic protein 1	ear1	30.5*	—	—	162.9*	—	—	9.3*	—
Eosinophil cationic protein 2	ear2	25.6*	—	29.4*	111.1*	—	—	8.5*	—
C-type lectins domain family	clec1a	—	—	—	—	—	—	−5.4*	—
Tetranectin	clec3b	—	—	2.6*	—	—	−3.0*	—	—
Dectin-1	clec7a	NC*	—	—	—	14.6*	—	—	—
C-type lectin domain family	clec10a	NC*	—	44.7*	38.6*	—	—	17.5*	—
C-type lectin domain family	clec14a	—	—	—	—	—	−6.7*	−3.3*	—
Surfactant protein A	sftpa	2.1*	—	3.1*	6.0*	—	−2.2*	—	—
Surfactant protein D	sftpd	—	—	—	—	—	−3.0*	—	—
HIC									
Chitinase-like protein	chil3	−2.2*	—	—	—	—	—	—	—
Chitinase-like protein	chil4	—	—	—	—	—	—	—	—
Galectin-3	lgals3	−4.7*	−2.6*	—	—	—	−2.2*	—	—
Von Willebrand factor	vWF	−2.3*	−2.3*	—	—	—	−2.2*	—	—
Resistin-like α	retnla	—	—	—	—	—	—	—	—
Macrophage mannose receptor 1	mrc1	—	−2.8*	—	—	—	−3.5*	—	—
Eosinophil cationic protein 1	ear1	−7.3*	—	—	—	—	−15.8*	—	—
Eosinophil cationic protein 2	ear2	−8.0*	—	—	—	—	—	—	—
C-type lectins domain family	clec1a	−2.3*	—	—	—	—	—	−2.2*	—
Tetranectin	clec3b	—	−2.3*	—	—	—	−3.2*	—	—
Dectin-1	clec7a	—	—	—	—	—	−4.8*	—	—
C-type lectin domain family	clec10a	—	—	—	—	—	—	—	—
C-type lectin domain family	clec14a	−2.7*	−3.7*	—	2.2*	—	—	—	—
Surfactant protein A	sftpa	−6.4*	−2.2*	—	—	—	−2.4*	—	—
Surfactant protein D	sftpd	−14.0*	−5.6*	—	—	—	−5.0*	—	—

Definition of abbreviations: HIC = heat-inactivated *Stachybotrys chartarum* conidia; NC = protein was detected in exposure group but not in air-only control group.
Values are reported as fold change between the exposed group and the air-only control group. Dashes indicate unchanged protein expression.
*$P \leq 0.05$; $n = 3$.

involving the proteins altered after strain A exposure were the hematological system development and function, as well as immune cell trafficking and tissue morphology. The top cardiotoxicity pathways included cardiac enlargement, dysfunction, and fibrosis.

The core proteomic analysis identified eIF2 signaling as well as mitochondrial dysfunction and cytidine diphosphate (CDP)-diacylglycerol biosynthesis I as the top canonical pathways associated with the proteins altered after exposure to strain B (Tables 3 and 4). CDP-diacylglycerol biosynthesis results in the synthesis of CDP-diacylglycerol, which is an intermediate product in the synthesis of cardiolipin, a phospholipid primarily located in the inner mitochondrial membrane. After 13 weeks of exposure to strain B, $G_{\beta\gamma}$ signaling, a contributor to heart failure and inflammation, was one of the top canonical pathways identified. In addition, organismal injury and abnormalities and inflammatory response were among the top diseases and disorders associated with the proteins altered after exposure to strain B.

Gene Expression Profiles

The RT^2 Profiler plates (Qiagen) measured genes involved in the Th1, Th2, or Th17 response pathways. Heat maps illustrate fold changes between viable exposed groups versus the air-only control group for both time points after 4-week and 13-week exposures (Figures 5 and 6). The majority of differentially expressed genes associated with Th1/Th2 immune responses were upregulated after strains A and B exposure (Figure 5), although not to the same extent. Many Th17-associated genes were downregulated after strain A versus strain B exposure (Figure 6). Overall, the Th1/Th2 and Th17 gene expression profiles were altered to a greater extent in lungs from strain A–exposed mice than in those from strain B–exposed mice.

Genes involved in tissue remodeling and the inflammatory response were increased after 4-week and 13-week strain A exposures, such as *retnla*, *chil3*, *arg1* (arginase 1), and *mrc1* (Table 5). These genes were upregulated after 13-week strain B exposure, but not to the extent of strain A. HIC exposure did not alter *retnla* and *chil3* expression by either strain; however,

Table 3. Strain A and Strain B 4-Week Exposure: Proteomic Core Analysis Summary Report Generated Using Ingenuity Pathway Analysis

	Strain A		Strain B	
4 wk	**24 h**	**48 h**	**24 h**	**48 h**
Canonical pathways	Oxidative phosphorylation (2.8×10^{-22}) Mitochondrial damage (9.1×10^{-22})	eIF2 signaling (4.4×10^{-04}) Antigen presentation pathway (1.6×10^{-03})	Mitochondrial dysfunction (1.1×10^{-02}) CDP-diacylglycerol biosynthesis I (7.6×10^{-03})	eIF2 signaling (1.3×10^{-25}) Integrin signaling (1.6×10^{-26})
Diseases and disorders	Organismal injury and abnormalities (1.3×10^{-02} to 1.2×10^{-15}) Inflammatory response (1.3×10^{-02} to 1.4×10^{-07})	Organismal injury and abnormalities (3.6×10^{-02} to 5.1×10^{-06}) Neurological disease (3.6×10^{-02} to 2.2×10^{-04})	Inflammatory response (4.8×10^{-02} to 5.0×10^{-03}) Immunological disease (1.6×10^{-02} to 1.2×10^{-03})	Organismal injury and abnormalities (1.2×10^{-04} to 6.9×10^{-35}) Inflammatory response (8.9×10^{-05} to 2.1×10^{-11})
Physiological system development and function	Tissue morphology (1.3×10^{-02} to 5.3×10^{-07}) Hematological system development and function (1.3×10^{-02} to 1.4×10^{-07}) Immune cell trafficking (1.1×10^{-02} to 1.4×10^{-07})	Hematological system development and function (3.6×10^{-02} to 3.2×10^{-04}) Lymphoid tissue structure and development (3.6×10^{-02} to 3.2×10^{-04}) Cell-mediated immune response (1.8×10^{-02} to 3.2×10^{-04})	Organismal development (4.8×10^{-02} to 2.9×10^{-04}) Tissue development (3.3×10^{-03} to 2.9×10^{-04}) Organ development (4.3×10^{-02} to 2.9×10^{-04})	Organismal survival (9.5×10^{-05} to 1.5×10^{-29}) Cardiovascular system development and function (8.9×10^{-05} to 1.6×10^{-17}) Tissue development (1.1×10^{-04} to 1.7×10^{-18})
Cardiotoxicity	Cardiac enlargement (5.2×10^{-01} to 2.2×10^{-02}) Cardiac dysfunction (1.0×10^{00} to 8.0×10^{-03}) Cardiac proliferation (1.7×10^{-01} to 2.2×10^{-02})	Cardiac fibrosis (4.4×10^{-01} to 2.9×10^{-01}) Cardiac enlargement (1.1×10^{00} to 8.8×10^{-02}) Cardiac damage (5.8×10^{-02} to 5.4×10^{-02})	Cardiac enlargement (2.8×10^{-01} to 5.5×10^{-03}) Cardiac dysfunction (2.0×10^{-01} to 4.8×10^{-02}) Cardiac inflammation (1.8×10^{-01} to 1.8×10^{-01})	Cardiac enlargement (5.1×10^{-01} to 5.1×10^{-05}) Cardiac fibrosis (5.8×10^{-01} to 1.4×10^{-05}) Cardiac damage (9.1×10^{-02} to 7.6×10^{-05})

Definition of abbreviations: CDP = cytidine diphosphate; eIF2 = eukaryotic initiation factor 2.
P values associated with each pathway/disease are shown in parentheses.

arg1 and *mrc1* were slightly upregulated after 4-week strain A HIC exposure. Monocyte chemoattractant protein 1, or *ccl2*, was also significantly increased after 4-week and 13-week strain A exposures (Figure 6), but it was only significantly increased after 13-week strain B exposure.

Strain A increased *il13* at both time points after 4 weeks, together with *il4* and *il6* at 48 hours. After 13-week strain A exposure, *ifng* (IFN-γ), *il2*, and *il13* expression was increased at both time points, *il4* and *il6* expression was increased at 48 hours (Figures 5 and 6). In contrast, strain B–exposed mice showed upregulated *il6* expression, together with significantly increased *il13* expression, after 4 weeks. After 13 weeks, *ifng* expression was slightly increased, together with significantly upregulated *il13* and *il5* at 24 hours and increased *il6* at 48 hours (Figures 5 and 6).

Involved with eosinophil recruitment, *il33* expression was initially upregulated after 4-week and 13-week strain A exposures compared with only after 13-week strain B exposure (Table 5). *Ccl7* (monocyte chemotactic protein 3) and *ccr3* were upregulated after 4-week and 13-week strain A exposures (Figure 5). Strain B exposure resulted in increased *ccl7* expression 48 hours after 4-week exposure and 24 hours after 13-week exposure (Figure 5). Inflammatory mediator *cxcl5* (Chemokine [C-X-C motif] ligand 5) and *cxcl1* expression was significantly increased after 4-week and 13-week strain A exposures (Figure 6). In strain B–exposed mice, *cxcl1* and *cxcl5* were upregulated 48 hours after 4 weeks, but not significantly. After 13 weeks, *cxcl1* was significantly upregulated (Figure 6).

miRNA Profiles

miRNA profiling analysis identified 531 (strain A) and 512 (strain B) miRNAs in the lung samples (Table E4). After 4-week strain A exposure, 116 (24 h) and 138 (48 h) miRNAs were significantly altered compared with air-only controls. After 13-week strain A exposure, 15 (24 h) and 49 (48 h) miRNAs were significantly differentially expressed, the majority of which were downregulated (Table E4). In contrast, no miRNAs were altered after 4-week strain B exposure, and only 14 (24 h) and 35 (48 h) miRNAs were differentially expressed after 13 weeks.

Using IPA, the miRNA target filter predicts miRNAs and target genes included

Table 4. Strain A and Strain B 13-Week Exposure: Proteomic Core Analysis Summary Report Generated Using Ingenuity Pathway Analysis

	Strain A		Strain B	
13 wk	**24 h**	**48 h**	**24 h**	**48 h**
Canonical pathways	eIF2 signaling (1.4×10^{-30}) Protein ubiquitination (1.0×10^{-19})	eIF2 signaling (2.2×10^{-42}) Mitochondrial dysfunction (1.1×10^{-29})	$G_{\beta\text{-}\gamma}$ signaling (9.3×10^{-08}) Integrin signaling (2.5×10^{-07})	eIF2 signaling (4.5×10^{-25}) Mitochondrial dysfunction (1.6×10^{-18})
Diseases and disorders	Organismal injury and abnormalities (7.3×10^{-03} to 4.0×10^{-31}) Inflammatory response (7.3×10^{-03} to 1.3×10^{-09})	Organismal injury and abnormalities (1.2×10^{-03} to 3.6×10^{-39}) Inflammatory response (1.1×10^{-03} to 3.5×10^{-11})	Organismal injury and abnormalities (7.6×10^{-03} to 1.6×10^{-06}) Cardiovascular disease (7.5×10^{-03} to 1.6×10^{-06})	Organismal injury and abnormalities (5.4×10^{-03} to 5.4×10^{-28}) Inflammatory response (4.6×10^{-03} to 2.3×10^{-08})
Physiological system development and function	Hematological system development and function (7.3×10^{-03} to 5.5×10^{-06}) Tissue morphology (6.6×10^{-03} to 8.9×10^{-06}) Immune cell trafficking (7.3×10^{-03} to 5.6×10^{-06})	Hematological system development and function (1.3×10^{-03} to 2.1×10^{-09}) Immune cell trafficking (1.3×10^{-03} to 2.2×10^{-09}) Tissue development (1.3×10^{-03} to 5.6×10^{-07})	Organismal development (6.9×10^{-03} to 1.8×10^{-09}) Cardiovascular system development and function (7.6×10^{-03} to 9.6×10^{-08}) Tissue morphology (7.6×10^{-03} to 1.3×10^{-06})	Hematological system development and function (4.7×10^{-03} to 3.2×10^{-09}) Tissue morphology (5.3×10^{-03} to 9.3×10^{-09}) Lymphoid tissue structure and development (4.6×10^{-03} to 9.3×10^{-09})
Cardiotoxicity	Cardiac infarction (5.1×10^{-05} to 5.1×10^{-05}) Cardiac dysfunction (4.7×10^{-01} to 9.5×10^{-03}) Cardiac inflammation (3.1×10^{-01} to 9.1×10^{-03})	Cardiac enlargement (4.6×10^{-01} to 7.9×10^{-04}) Cardiac fibrosis (5.4×10^{-01} to 2.8×10^{-03}) Cardiac dysfunction (3.6×10^{-01} to 3.5×10^{-04})	Cardiac fibrosis (4.5×10^{-01} to 1.1×10^{-03}) Cardiac inflammation (1.8×10^{-01} to 1.0×10^{-02}) Cardiac damage (1.4×10^{-01} to 1.8×10^{-03})	Cardiac enlargement (5.3×10^{-01} to 1.3×10^{-03}) Cardiac dysfunction (2.9×10^{-01} to 2.5×10^{-02}) Heart failure (4.9×10^{-01} to 2.8×10^{-02})

P values associated with each pathway/disease are shown in parentheses.

in this study. A regulator of *il13* and *il33*, miR-339-5p was decreased after strain A and strain A HIC exposures (Table 6). Downregulation of miR-365 after 4-week strain A viable and HIC exposure was predicted to regulate *il6*. Expression of *il10* was predicted to increase due to decreased miR-144-5p or miR-374b-5p expression after strain A viable and HIC exposure. After strain B viable and HIC exposure, the expression of these miRNAs was unchanged (Table 6). Expression of Th1 cytokines, such as *il2* and *tnf*, may be regulated by miR-181b-5p (*il2*), miR-21a-5p (*tnf*), and miR-669d-5p (*tnf*). miR-181b-5b was decreased after 4-week strain A exposure and at 4-week and 13-week strain A HIC exposure. miR-21a-5p was upregulated only after 13-week strain A exposure, but it was downregulated 24 hours after 13-week strain A HIC exposure. After strain A viable and HIC exposure, miR-669d-5p expression was increased. After strain B viable and HIC exposure, the expression of these miRNAs was unchanged. Critical to eosinophilic recruitment, miR-133a-3p and miR-335-5p were downregulated after strain A viable and HIC exposure, but unchanged after strain B exposure. miR-23b-3p, a regulator of *arg1* and *mrc1*, was downregulated after strain A exposure, but not after HIC exposure. In contrast to downregulation after 13-week strain B exposure, miR-23b-3p was unchanged after HIC exposure.

Discussion

The results of this study showed that repeated exposure to *S. chartarum* results in inflammation and pulmonary arterial remodeling. The molecular and immunological markers underlying the inflammatory response, as well as the rate at which the remodeling occurred, varied between the two strains. Strain A, the higher-fragmenting strain, elicited an earlier Th2-mediated immune response after 4 weeks that shifted to a mixed T-cell response after 13 weeks. Arterial remodeling after strain A exposure was observed at an earlier time point than in mice exposed to the lower-fragmenting strain B; however, arterial remodeling was evident after 13 weeks of exposure to both strains. After 4 weeks, strain B exposure also elicited a pulmonary Th2 immune response, which remained after 13 weeks. Although HIC exposure did not result in significant lung pathology, alterations in

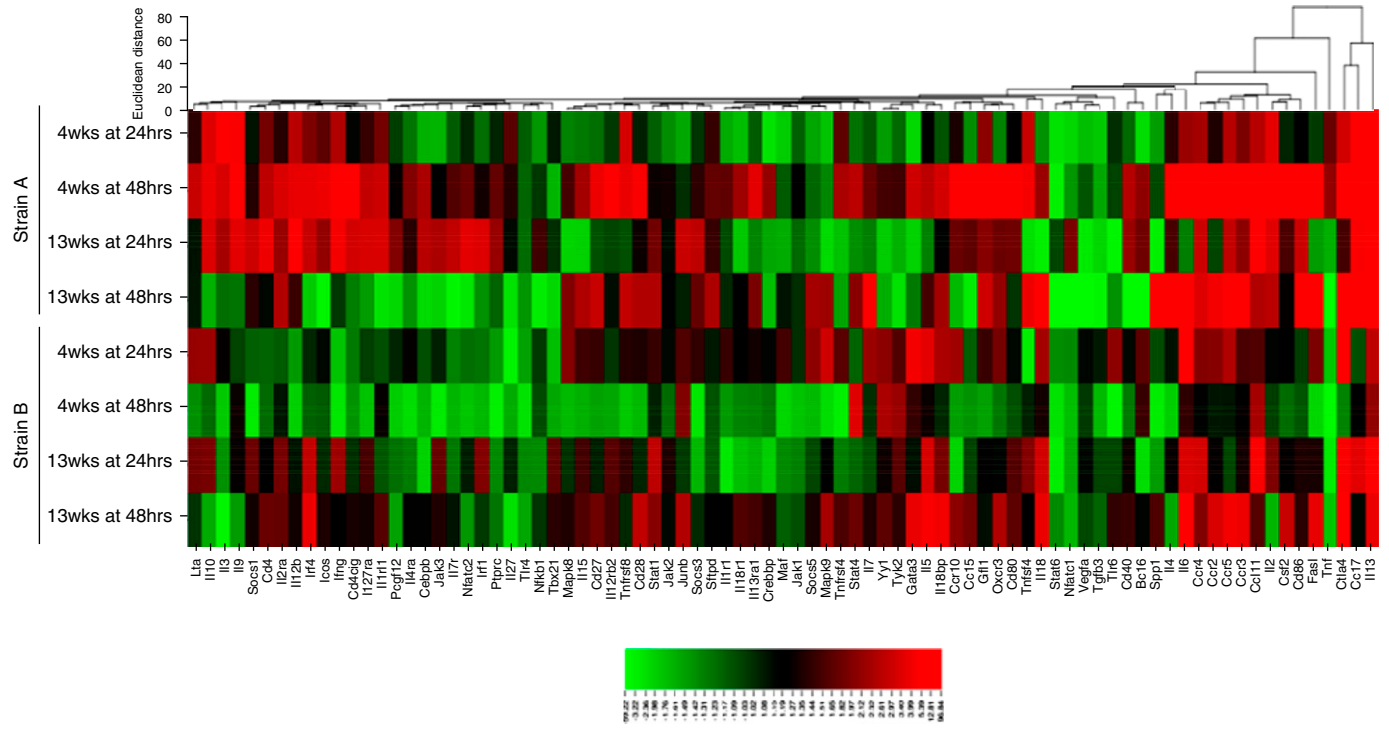

Figure 5. Heat map of genes involved in the T-helper cell type 1 (Th1) and Th2 immune response pathways. Altered genes involved in the Th1 and Th2 response pathways after 4 weeks and 13 weeks of exposure to strain A and to strain B. Genes are color coded (red and green for up- and downregulation, respectively) and are arranged by Euclidean distance; $n = 3–5$ per group.

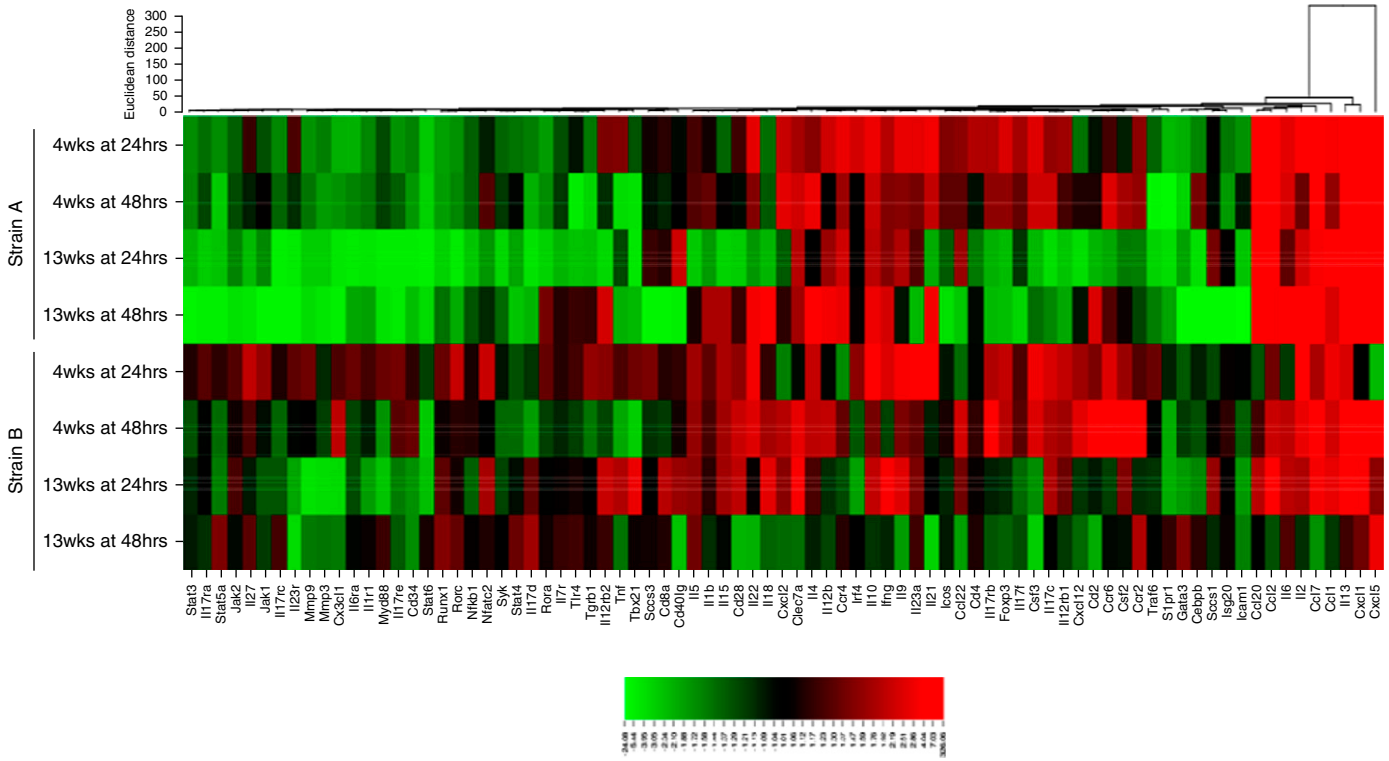

Figure 6. Heat map of genes involved in the Th17 immune response pathway. Altered genes involved in the Th17 response pathways after 4-week and 13-week exposures to strain A and to strain B. Genes are color coded (red and green for up- and downregulation, respectively) and are arranged by Euclidean distance; $n = 3–5$ per group.

Table 5. Differentially Expressed Genes after Exposure

Genes	Symbol	Strain A 4 wk 24 h	Strain A 13 wk 48 h	Strain B 4 wk 24 h	Strain B 13 wk 48 h	Strain A 4 wk 24 h	Strain A 13 wk 48 h	Strain B 4 wk 24 h	Strain B 13 wk 48 h
Viable									
Arginase-1	*arg1*	13.4*	12.5*	3.8	9.8*	—	—	6.0*	2.1
Cluster of differentiation 163	*cd163*	—	—	—	8.9*	−2.6	—	—	—
Cluster of differentiation 163	*cd163*	—	—	—	67.3*	—	—	—	—
Chitinase-like 3	*chil3*	20.9*	15.0*	81.8*	—	−2.3	2.8*	32.1*	—
C-type lectin domain family 4(n)	*clec4n*	2.2*	—	5.1*	—	−3.8*	—	—	—
Interleukin-33	*il33*	3.9*	2.8*	5.2*	—	—	—	4.8*	—
Mannose receptor	*mrc1*	5.8*	—	4.2*	—	—	—	3.8*	−6.0
Resistin-like α	*retnla*	247.6*	60.6*	145.1*	−3.9	9.0*	39.0*	108.2*	−3.5
Thymic stromal lymphopoietin	*tslp*	3.3*	−2.6	—	—	−3.4*	−2.2*	7.1*	—
HIC									
Arginase-1	*arg1*	4.8*	—	—	3.0	—	−4.3*	2.6	—
C-C chemokine receptor 7	*ccr7*	—	—	—	2.2	—	—	—	—
Cluster of differentiation 163	*cd163*	2.5*	—	4.0*	3.0	—	—	—	2.3
Chitinase-like 3	*chil3*	—	—	—	−4.0*	—	−2.1	—	—
C-type lectin domain family 4(n)	*clec4n*	—	—	—	—	—	—	—	—
Interleukin-33	*il33*	—	—	−2.8*	−3.8	—	—	—	—
Mannose receptor	*mrc1*	2.1*	—	—	—	—	—	—	−4.1
Resistin-like α	*retnla*	—	—	—	—	2.3	—	—	−3.8*
Thymic stromal lymphopoietin	*tslp*	3.1*	—	—	—	2.0	—	—	—

Values are reported as fold change between the exposed group compared with air-only control group. Dashes indicate unchanged gene expression.
*$P \leq 0.05$; $n = 3$–5.

protein, gene, and miRNA profiles were evident, suggesting a unique fungus-induced profile, regardless of viability. Neither viable strain B nor either HIC strain generated as many fragments as viable strain A; therefore, mice exposed to viable strain A fragments inhaled a greater number of smaller particles, resulting in less mass deposition within the lungs of these mice than in mice exposed to strain B or to either strain of HIC. This difference in exposure suggests that exposure to fungal fragments, despite decreased pulmonary mass deposition, elicits an earlier pulmonary immune response and pathology after repeated *S. chartarum* exposure.

Using the same concentration of *S. chartarum* as in the present study, Ochiai and colleagues also reported that repeated intratracheal instillations of *S. chartarum* resulted in pulmonary arterial hypertension (PAH) as early as 4 weeks (24). In the present study, histopathology showed pulmonary arterial remodeling after strains A and B exposure; however, arterial remodeling developed earlier with strain A than with strain B. In another study of repeated intratracheal instillations of *S. chartarum*, goblet cell metaplasia was observed after seven exposures, but not after a single exposure, indicative of airway remodeling after *S. chartarum* exposure (25). In agreement with Fan and colleagues, retnla was increased with arterial remodeling, together with asthma pathogenesis and tissue remodeling–associated proteins (32). These proteins and respective genes were significantly increased after both viable *S. chartarum* exposures compared with air-only and HIC controls, as well as at an earlier time point in strain A–exposed versus strain B–exposed mice. A potential protein biomarker for PAH, lgals3 (33), and *ccl2*, involved in pulmonary inflammation and vascular tissue remodeling, were upregulated after 4-week and 13-week strain A exposures, but only after 13-week strain B exposure. Proteomic core analysis indicated associations with inflammatory responses, tissue remodeling, and cardiac abnormalities after exposure to both strains (Tables 3 and 4). Highly affected canonical pathways, such as mitochondrial dysfunction (34) and pathways contributing to heart failure (35, 36) and inflammation (37), suggested that the pulmonary vasculature may be affected after fungal exposures. Pulmonary arterial remodeling is a Th2-mediated response (13, 30, 38) and is in agreement with the Th2-mediated immune response observed in this study, as well as in other studies of repeated exposure to *S. chartarum* (25, 30). The resultant pulmonary arterial remodeling progressed at strain-specific rates, which is further supported by gene and proteomic alterations.

Increased *il13*, *il4*, and *il5* gene expression, together with no significant *ifng* or *tnf* increase, after 4-week strains A and B exposures indicates a Th2-mediated immune response. Interestingly, 13-week strain B exposure maintained the Th2-dominant response, whereas strain A exposure shifted to a mixed T-cell response. A limitation of our study was that, for unknown reasons, the cycle threshold values for genes from HIC-exposed lungs were reported as undetermined after RT-PCR. Differential staining of BALF cells collected from strain A– and strain B–exposed mice supported *il4* gene expression data (not shown); however, BALF volume limited the measurement of IL-13. In another study, increased eosinophils, IL-4, and IL-5, but not IFN-γ, were observed in BALF after intratracheal instillation for 12 weeks (30), which agreed with strain B but differed from strain A. Taken together, the results suggest that different strains of *S. chartarum* elicit a continuum of immune response, dependent on the duration and composition of exposure.

Histology and BALF collected from *S. chartarum*–exposed mice showed the

Table 6. Altered MicroRNAs after Exposure

	Strain A		Strain B		Strain A		Strain B	
	4 wk	13 wk	4 wk	13 wk	4 wk	13 wk	4 wk	13 wk
miRNAs	24 h	48 h	24 h	48 h	24 h	48 h	24 h	48 h
Viable								
mmu-miR-133a-3p	−3.2*	−3.0*	−3.3*	−2.4*	—	—	—	−2.3
mmu-miR-144-5p	−2.2*	−2.1*	−2.2*	−3.0*	—	—	—	—
mmu-miR-181b-5p	−2.2*	−2.1*	—	—	—	—	—	—
mmu-miR-21a-5p	—	—	2.9*	1.9*	—	—	—	—
mmu-miR-23b-3p	−3.4*	−2.3*	—	−2.1*	—	—	−2.0*	—
mmu-miR-335-5p	−2.2*	−2.7*	—	−2.3	—	—	—	—
mmu-miR-339-5p	−2.0*	−2.9*	−2.0*	−2.4*	—	—	—	—
mmu-miR-365-3p	−2.2*	−2.4*	—	−1.7*	—	—	—	—
mmu-miR-374b-5p	−2.2*	−2.3*	—	−2.0*	—	—	—	−1.8*
mmu-miR-491-3p	—	3.0*	—	2.2*	—	—	−1.7*	—
mmu-miR-669d-5p	2.7*	2.8*	—	2.0*	—	—	—	—
mmu-miR-706	4.7*	7.4*	2.2*	3.2*	—	—	—	2.1*
HIC								
mmu-miR-133a-3p	−4.2*	−3.4*	−5.9*	−3.2*	—	2.1	—	—
mmu-miR-144-5p	—	—	−4.4*	−2.3*	—	—	—	—
mmu-miR-181b-5p	−2.7*	−2.4*	−3.1*	−2.2*	—	—	—	—
mmu-miR-21a-5p	—	—	−3.1*	—	—	—	—	—
mmu-miR-23b-3p	−1.9*	—	—	—	—	—	—	—
mmu-miR-335-5p	−2.8*	−2.3*	−3.0*	−2.3*	—	—	—	—
mmu-miR-339-5p	−2.2*	−2.4*	−3.3*	−2.5*	—	—	—	—
mmu-miR-365-3p	−4.3*	−3.6*	−4.6*	−3.2*	—	—	—	—
mmu-miR-374b-5p	−2.3*	−2.0*	−3.3*	−2.1*	—	—	—	—
mmu-miR-491-3p	2.7*	5.9*	3.3*	3.9*	—	—	—	—
mmu-miR-669d-5p	3.6*	3.1*	3.9*	2.4*	—	—	—	—
mmu-miR-706	7.4*	7.5*	6.3*	3.7*	—	—	—	—

Definition of abbreviations: miR and miRNA = microRNA.
Values are reported as fold change between the exposed group compared with air-only control group. Dashes indicate miRNA was unaltered.
*$P \leq 0.05$; $n = 5$.

presence of eosinophils, neutrophils, and macrophages. In agreement with the present study, a study comparing a single intratracheal instillation of *S. chartarum* spores with multiple instillations (once per week for 7 wk) showed increased lymphocytes and eosinophils after multiple exposures (25). Released during degranulation of eosinophils, ear1 and ear2 were significantly increased after 4-week and 13-week strain A exposures, compared with only 13-week strain B exposure. Critical to eosinophil commitment, IL-5 is preceded by IL-33 (39), both of which were upregulated after both 4-week and 13-week strain A exposures compared with only after 13-week strain B exposure. Having eosinophilic chemoattractant properties, *ccl7* and *ccr3* were upregulated after strain A exposure. Eosinophils produce cxcl5, which, together with cxcl1, attracts neutrophils (40). Exposure to both strains resulted in a temporal increase in *cxcl5* and *cxcl1* expression, indicative of the progressive influx of pulmonary neutrophils. Associated with alternatively activated macrophages, *arg1* and *mrc1* were upregulated after exposure to both strains. Together with other increased M2 markers such as *retnla*, *chil3*, and *il33* (41–43), these data correlate with increased macrophages observed in exposed lungs. Overall, the results support the increased presence of inflammatory cell infiltrates and the earlier induction of an immune response after strain A versus strain B exposure.

Clec proteins are critical in the recognition and neutralization of pathogens (44). Exposure to both strains increased clec7a protein expression after 4-week exposure. Gene expression was increased after 4-week strain A and 13-week strain B exposures. Although *S. chartarum* spores are too large to deposit deep within the lung and subsequently germinate, previous studies highlighted the association between increased clec7a expression with germination after *A. fumigatus* exposure (28, 29). In addition, gene expression analyses showed increased *clec4n* after 4-week and 13-week strain A exposures, with decreased expression after 4-week strain B exposure. Mrc1 also contributes to pathogen recognition by recognizing complex carbohydrates (45). Together, increased expression of proteins involved in pathogen recognition supports the hypothesis that fungal fragments enter the lung and elicit an immune response.

Increased gene expression associated with decreased expression of regulating miRNAs suggests a possible mechanism underlying the immune response after *S. chartarum* exposure. Using the same delivery system, altered miRNAs after *A. fumigatus* exposure (28) were also found to be altered in the present study (Table 6). miR-23b-3p, one of the highest-altered miRNAs after *A. fumigatus* exposure, was also altered after *S. chartarum* exposure. In *A. fumigatus*–exposed mice, mir-706 expression was increased (28); however, after strain A exposure, miR-706 consistently had the highest fold change for all time points, except 24 hours after 13 weeks, when miR-21a-5p expression was highest (Table 6). miR-706 is involved in liver fibrogenesis (46); however, the present results also suggest involvement in pulmonary tissue remodeling. In agreement with the present study, miR-21a is involved in pulmonary fibrogenesis (47) and was surprisingly decreased after *A. fumigatus* exposure (28). The difference in miR-21a expression is most likely due to the difference in fungal species; however, research suggests that *A. fumigatus* elicits an immune response due to fungal germination (28, 29), whereas this study suggests the earlier induction of an immune response is driven by the fungal fragments present in greater numbers in the composition of strain A exposure.

The repeated fungal exposure model presented in this study reproducibly elicited pulmonary arterial remodeling in both *S. chartarum* strains. Other studies that have induced PAH through well-known mechanisms, such as hypoxic conditions or monocrotaline injury, have several limitations, as discussed by Provencher and colleagues (48), including less stringent study designs. The model in the present study appears to overcome several of the described methodological limitations (48, 49); however, future

studies focusing on critical parameters required to identify PAH, such as cardiac measurements and pulmonary artery smooth muscle thickness, will need to be conducted to better understand the initiation and recovery of PAH using fungal test articles such as *S. chartarum*.

Respiratory morbidities in patients exposed to *S. chartarum* have been reported (50, 51), highlighting the importance of characterizing mechanisms influencing the pulmonary immune response and disease pathology. Published studies have identified fungal particles aerosolized from moldy building materials (52, 53), but those studies were unable to isolate and characterize the effect of individual fungal species. Having different mycotoxin profiles, both *A. fumigatus* (29) and *S. chartarum* induce pulmonary arterial remodeling; therefore, it appears more likely that common fungal antigens present on the respirable *S. chartarum* fragments are inducing the early pathophysiological response. Collectively, the results of this study demonstrate that exposure to *S. chartarum* elicits pulmonary immune responses and pulmonary arterial remodeling; however, it is the presence of fungal fragments that induces these responses. ■

Author disclosures are available with the text of this article at www.atsjournals.org.

Acknowledgment: The authors acknowledge Benjamin P. Jackson, M.D., NIOSH, for his contribution in fungal cultivation.

References

1. World Health Organization (WHO). WHO guidelines for indoor air quality: dampness and mould. Geneva, Switzerland: WHO Regional Office for Europe; 2009.
2. Institute of Medicine. Damp indoor spaces and health. Washington, DC: National Academies Press; 2004.
3. Montaña E, Etzel RA, Allan T, Horgan TE, Dearborn DG. Environmental risk factors associated with pediatric idiopathic pulmonary hemorrhage and hemosiderosis in a Cleveland community. *Pediatrics* 1997;99:e5.
4. Centers for Disease Control and Prevention (CDC). Acute pulmonary hemorrhage/hemosiderosis among infants: Cleveland, January 1993–November 1994. *MMWR Morb Mortal Wkly Rep* 1994;43: 881–883.
5. Centers for Disease Control and Prevention (CDC). Update: pulmonary hemorrhage/hemosiderosis among infants—Cleveland, Ohio, 1993–1996. *MMWR Morb Mortal Wkly Rep* 2000;49: 180–184.
6. Pestka JJ, Yike I, Dearborn DG, Ward MD, Harkema JR. *Stachybotrys chartarum*, trichothecene mycotoxins, and damp building-related illness: new insights into a public health enigma. *Toxicol Sci* 2008;104: 4–26.
7. Andersson MA, Nikulin M, Köljalg U, Andersson MC, Rainey F, Reijula K, *et al*. Bacteria, molds, and toxins in water-damaged building materials. *Appl Environ Microbiol* 1997;63:387–393.
8. Boutin-Forzano S, Charpin-Kadouch C, Chabbi S, Bennedjai N, Dumon H, Charpin D. Wall relative humidity: a simple and reliable index for predicting *Stachybotrys chartarum* infestation in dwellings. *Indoor Air* 2004;14:196–199.
9. Brasel TL, Martin JM, Carriker CG, Wilson SC, Straus DC. Detection of airborne *Stachybotrys chartarum* macrocyclic trichothecene mycotoxins in the indoor environment. *Appl Environ Microbiol* 2005; 71:7376–7388.
10. Jarvis BB, Sorenson WG, Hintikka EL, Nikulin M, Zhou Y, Jiang J, *et al*. Study of toxin production by isolates of *Stachybotrys chartarum* and *Memnoniella echinata* isolated during a study of pulmonary hemosiderosis in infants. *Appl Environ Microbiol* 1998;64:3620–3625.
11. Barnes C, Buckley S, Pacheco F, Portnoy J. IgE-reactive proteins from *Stachybotrys chartarum*. *Ann Allergy Asthma Immunol* 2002;89: 29–33.
12. Chung YJ, Copeland LB, Doerfler DL, Ward MD. The relative allergenicity of *Stachybotrys chartarum* compared to house dust mite extracts in a mouse model. *Inhal Toxicol* 2010; 22:460–468.
13. Yike I, Dearborn D. Guest editorial: novel insights into the pathology of *Stachybotrys chartarum*. *Mycopathologia* 2011;172: 1–3.
14. Rand TG, Sun M, Gilyan A, Downey J, Miller JD. Dectin-1 and inflammation-associated gene transcription and expression in mouse lungs by a toxic (1,3)-β-D glucan. *Arch Toxicol* 2010;84: 205–220.
15. Vesper SJ, Magnuson ML, Dearborn DG, Yike I, Haugland RA. Initial characterization of the hemolysin stachylysin from *Stachybotrys chartarum*. *Infect Immun* 2001;69:912–916.
16. Miller JD, Sun M, Gilyan A, Roy J, Rand TG. Inflammation-associated gene transcription and expression in mouse lungs induced by low molecular weight compounds from fungi from the built environment. *Chem Biol Interact* 2010;183:113–124.
17. Górny RL, Reponen T, Willeke K, Schmechel D, Robine E, Boissier M, *et al*. Fungal fragments as indoor air biocontaminants. *Appl Environ Microbiol* 2002;68:3522–3531.
18. Cho SH, Seo SC, Schmechel D, Grinshpun SA, Reponen T. Aerodynamic characteristics and respiratory deposition of fungal fragments. *Atmos Environ* 2005;39:5454–5465.
19. Green BJ, Tovey ER, Sercombe JK, Blachere FM, Beezhold DH, Schmechel D. Airborne fungal fragments and allergenicity. *Med Mycol* 2006;44 (Suppl 1):S245–S255.
20. Yike I, Rand TG, Dearborn DG. Acute inflammatory responses to *Stachybotrys chartarum* in the lungs of infant rats: time course and possible mechanisms. *Toxicol Sci* 2005;84:408–417.
21. Rao CY, Burge HA, Brain JD. The time course of responses to intratracheally instilled toxic *Stachybotrys chartarum* spores in rats. *Mycopathologia* 2000;149:27–34.
22. Rand TG, Mahoney M, White K, Oulton M. Microanatomical changes in alveolar type II cells in juvenile mice intratracheally exposed to *Stachybotrys chartarum* spores and toxin. *Toxicol Sci* 2002;65: 239–245.
23. Korpi A, Kasanen JP, Raunio P, Kosma VM, Virtanen T, Pasanen AL. Effects of aerosols from nontoxic *Stachybotrys chartarum* on murine airways. *Inhal Toxicol* 2002;14:521–540.
24. Ochiai E, Kamei K, Watanabe A, Nagayoshi M, Tada Y, Nagaoka T, *et al*. Inhalation of *Stachybotrys chartarum* causes pulmonary arterial hypertension in mice. *Int J Exp Pathol* 2008;89:201–208.
25. Rosenblum Lichtenstein JH, Molina RM, Donaghey TC, Hsu YH, Mathews JA, Kasahara DI, *et al*. Repeated mouse lung exposures to *Stachybotrys chartarum* shift immune response from type 1 to type 2. *Am J Respir Cell Mol Biol* 2016;55:521–531.
26. Leino MS, Alenius HT, Fyhrquist-Vanni N, Wolff HJ, Reijula KE, Hintikka EL, *et al*. Intranasal exposure to *Stachybotrys chartarum* enhances airway inflammation in allergic mice. *Am J Respir Crit Care Med* 2006;173:512–518.
27. Buskirk AD, Green BJ, Lemons AR, Nayak AP, Goldsmith WT, Kashon ML, *et al*. A murine inhalation model to characterize pulmonary exposure to dry *Aspergillus fumigatus* conidia. *PLoS One* 2014;9: e109855.
28. Croston TL, Nayak AP, Lemons AR, Goldsmith WT, Gu JK, Germolec DR, *et al*. Influence of *Aspergillus fumigatus* conidia viability on murine pulmonary microRNA and mRNA expression following subchronic inhalation exposure. *Clin Exp Allergy* 2016;46: 1315–1327.
29. Nayak AP, Croston TL, Lemons AR, Goldsmith WT, Marshall NB, Kashon ML, *et al*. *Aspergillus fumigatus* viability drives allergic responses to inhaled conidia. *Ann Allergy Asthma Immunol* 2018; 121:200–210, e2.

30. Nagayoshi M, Tada Y, West J, Ochiai E, Watanabe A, Toyotome T, *et al*. Inhalation of *Stachybotrys chartarum* evokes pulmonary arterial remodeling in mice, attenuated by Rho-kinase inhibitor. *Mycopathologia* 2011;172:5–15.
31. Croston TL, Nayak AP, Lemons AR, Goldsmith WT, Germolec DM, Beezhold DH, *et al*. Pulmonary immune response following subchronic *Stachybotrys chartarum* exposure [abstract]. *J Allergy Clin Immunol* 2017;139(2 Suppl):AB75.
32. Fan C, Meuchel LW, Su Q, Angelini DJ, Zhang A, Cheadle C, *et al*. Resistin-like molecule α in allergen-induced pulmonary vascular remodeling. *Am J Respir Cell Mol Biol* 2015;53:303–313.
33. Calvier L, Legchenko E, Grimm L, Sallmon H, Hatch A, Plouffe BD, *et al*. Galectin-3 and aldosterone as potential tandem biomarkers in pulmonary arterial hypertension. *Heart* 2016;102:390–396.
34. Croston TL, Shepherd DL, Thapa D, Nichols CE, Lewis SE, Dabkowski ER, *et al*. Evaluation of the cardiolipin biosynthetic pathway and its interactions in the diabetic heart. *Life Sci* 2013; 93:313–322.
35. Williams ML, Hata JA, Schroder J, Rampersaud E, Petrofski J, Jakoi A, *et al*. Targeted β-adrenergic receptor kinase (βARK1) inhibition by gene transfer in failing human hearts. *Circulation* 2004;109:1590–1593.
36. Rockman HA, Chien KR, Choi DJ, Iaccarino G, Hunter JJ, Ross J Jr, *et al*. Expression of a β-adrenergic receptor kinase 1 inhibitor prevents the development of myocardial failure in gene-targeted mice. *Proc Natl Acad Sci USA* 1998;95:7000–7005.
37. Hirsch E, Katanaev VL, Garlanda C, Azzolino O, Pirola L, Silengo L, *et al*. Central role for G protein-coupled phosphoinositide 3-kinase γ in inflammation. *Science* 2000;287:1049–1053.
38. Daley E, Emson C, Guignabert C, de Waal Malefyt R, Louten J, Kurup VP, *et al*. Pulmonary arterial remodeling induced by a Th2 immune response. *J Exp Med* 2008;205:361–372.
39. Johnston LK, Hsu CL, Krier-Burris RA, Chhiba KD, Chien KB, McKenzie A, *et al*. IL-33 precedes IL-5 in regulating eosinophil commitment and is required for eosinophil homeostasis. *J Immunol* 2016;197: 3445–3453.
40. Qiu Y, Zhu J, Bandi V, Atmar RL, Hattotuwa K, Guntupalli KK, *et al*. Biopsy neutrophilia, neutrophil chemokine and receptor gene expression in severe exacerbations of chronic obstructive pulmonary disease. *Am J Respir Crit Care Med* 2003;168:968–975.
41. Murray PJ, Allen JE, Biswas SK, Fisher EA, Gilroy DW, Goerdt S, *et al*. Macrophage activation and polarization: nomenclature and experimental guidelines. *Immunity* 2014;41:14–20.
42. Bosurgi L, Cao YG, Cabeza-Cabrerizo M, Tucci A, Hughes LD, Kong Y, *et al*. Macrophage function in tissue repair and remodeling requires IL-4 or IL-13 with apoptotic cells. *Science* 2017;356: 1072–1076.
43. Mantovani A, Biswas SK, Galdiero MR, Sica A, Locati M. Macrophage plasticity and polarization in tissue repair and remodelling. *J Pathol* 2013;229:176–185.
44. Weis WI, Taylor ME, Drickamer K. The C-type lectin superfamily in the immune system. *Immunol Rev* 1998;163:19–34.
45. Stahl PD, Ezekowitz RAB. The mannose receptor is a pattern recognition receptor involved in host defense. *Curr Opin Immunol* 1998;10:50–55.
46. Yin R, Guo D, Zhang S, Zhang X. miR-706 inhibits the oxidative stress-induced activation of PKCα/TAOK1 in liver fibrogenesis. *Sci Rep* 2016;6:37509.
47. Rajasekaran S, Rajaguru P, Sudhakar Gandhi PS. MicroRNAs as potential targets for progressive pulmonary fibrosis. *Front Pharmacol* 2015;6:254.
48. Provencher S, Archer SL, Ramirez FD, Hibbert B, Paulin R, Boucherat O, *et al*. Standards and methodological rigor in pulmonary arterial hypertension preclinical and translational research. *Circ Res* 2018; 122:1021–1032.
49. Bonnet S, Provencher S, Guignabert C, Perros F, Boucherat O, Schermuly RT, *et al*. Translating research into improved patient care in pulmonary arterial hypertension. *Am J Respir Crit Care Med* 2017; 195:583–595.
50. Johanning E, Biagini R, Hull D, Morey P, Jarvis B, Landsbergis P. Health and immunology study following exposure to toxigenic fungi (*Stachybotrys chartarum*) in a water-damaged office environment. *Int Arch Occup Environ Health* 1996;68:207–218.
51. Hodgson MJ, Morey P, Leung WY, Morrow L, Miller D, Jarvis BB, *et al*. Building-associated pulmonary disease from exposure to *Stachybotrys chartarum* and *Aspergillus versicolor*. *J Occup Environ Med* 1998;40:241–249.
52. Madsen AM, Larsen ST, Koponen IK, Kling KI, Barooni A, Karottki DG, *et al*. Generation and characterization of indoor fungal aerosols for inhalation studies. *Appl Environ Microbiol* 2016;82:2479–2493.
53. Mensah-Attipoe J, Saari S, Veijalainen AM, Pasanen P, Keskinen J, Leskinen JTT, *et al*. Release and characteristics of fungal fragments in various conditions. *Sci Total Environ* 2016;547: 234–243.